

# Nonlinear free vibration and post-buckling of FG-CNTRC beams on nonlinear foundation

Hamed Shafiei<sup>a</sup> and Ali Reza Setoodeh<sup>\*</sup>

Department of Mechanical and Aerospace Engineering, Shiraz University of Technology, Shiraz 71555, Iran

(Received September 20, 2016, Revised February 27, 2017, Accepted March 10, 2017)

**Abstract.** The purpose of this research is to study the nonlinear free vibration and post-buckling analysis of functionally graded carbon nanotube reinforced composite (FG-CNTRC) beams resting on a nonlinear elastic foundation. Uniformly and functionally graded distributions of single walled carbon nanotubes as reinforcing phase are considered in the polymeric matrix. The modified form of rule of mixture is used to estimate the material properties of CNTRC beams. The governing equations are derived employing Euler-Bernoulli beam theory along with energy method and Hamilton's principle. Applying von Kármán's strain-displacement assumptions, the geometric nonlinearity is taken into consideration. The developed governing equations with quadratic and cubic nonlinearities are solved using variational iteration method (VIM) and the analytical expressions and numerical results are obtained for vibration and stability analysis of nanocomposite beams. The presented comparative results are indicative for the reliability, accuracy and fast convergence rate of the solution. Eventually, the effects of different parameters, such as foundation stiffness, volume fraction and distributions of carbon nanotubes, slenderness ratio, vibration amplitude, coefficients of elastic foundation and boundary conditions on the nonlinear frequencies, vibration response and post-buckling loads of FG-CNTRC beams are examined. The developed analytical solution provides direct insight into parametric studies of particular parameters of the problem.

**Keywords:** nanocomposites; functionally graded beams; nonlinear vibration; post-buckling loads; nonlinear elastic foundation

## 1. Introduction

Composite materials, due to their unique physical properties such as high stiffness to weight ratio, have obtained a wide range of applications in fabrication of engineering structures and are an attractive research area for scientists (Malekzadeh and Setoodeh 2007, Malekzadeh and Vosoughi 2009, Sahoo and Singh 2014, Biswal *et al.* 2016). For instance, Vosoughi *et al.* (2012) investigated thermal buckling and post-buckling of laminated composite beams applying the first-order shear deformation beam theory and differential quadrature method. A modified Fourier-Ritz approach was utilized by Wang *et al.* (2016) to study the free vibration of laminated composite beams. They assumed that the beam is subjected to an axial load and used a standard Fourier cosine series and several closed-form functions to state the displacements of the beam. Alesadi *et al.* (2017) employed Isogeometric approach along with Carrera's unified formulation to study free vibration and buckling of laminated composite plates. The higher-order functions for approximation of the field solution were applied by them to increase the accuracy of the investigation.

Carbon nanotubes (CNTs) were introduced by Iijima

(1991) in 1991. Afterwards, several studies on CNTs demonstrated that they have significant mechanical properties which make them suitable reinforcement for composite structures (Esawi and Farag 2007, Thostenson *et al.* 2001). So, carbon nanotube reinforced composites (CNTRCs) have been increasingly applied in various fields of science and technology, and meanwhile, many studies have been devoted to develop different approaches to examine mechanical behavior of related structures (Cadec *et al.* 2002, Fiedler *et al.* 2006, Sun *et al.* 2005). Han and Elliot (2007) employed classical molecular dynamics to simulate the elastic properties of polymer/carbon nanotube composite. Using a micromechanical approach, Thostenson and Chou (2003) showed that the size of CNTs influences the elastic properties of nanotube-based composites. Lu and Hu (2012) investigated mechanical properties of CNTs via computational simulations. They developed an improved 3D finite element model and studied different types of single-walled carbon nanotubes (SWCNTs). Wuite and Adali (2005) used a micromechanics model to analyze the deflection and stress behavior of CNTRC beams. Based on the Airy stress-function method, the pure bending and local buckling of a composite beam reinforced with SWCNTs was investigated by Vodenitcharova and Zhang (2006). Formica *et al.* (2010) conducted a research study on the vibrational properties of CNTRCs using an equivalent continuum model.

The most important issue in the analysis of nanostructures is applying the nanoscale effects

<sup>\*</sup>Corresponding author, Associate Professor,  
E-mail: setoodeh@sutech.ac.ir

<sup>a</sup> Graduate Student

(Malekzadeh and Dehbozorgi 2016, Anjana *et al.* 2016, Bağdatli 2015a, Togun and Bağdatli 2016a). In this regard, Shen (2009) presented a macro-mechanical model for bending of FG-CNTRCs which afterwards have been utilized extensively for bending, buckling and vibrational analysis of such nanocomposites (Mehrabadi *et al.* 2012, Zhu *et al.* 2012, Malekzadeh and Zarei 2014, Zafarmand and Kadkhodayan 2014, Malekzadeh and Heydarpour 2015, Setoodeh and Shojaee 2016, Jooybar *et al.* 2016, Heydarpour *et al.* 2014, Setoodeh and Shojaee 2017). Among them, some researchers have investigated vibration and buckling of FG-CNTRC beams. Ke *et al.* (2010a) utilized Timoshenko beam theory and von Kármán geometric nonlinearity to discuss the nonlinear free vibration of FG-CNTRC beams using Ritz method. Yas and Samadi (2012) examined free vibration and buckling of CNTRC Timoshenko beams. They assumed that the beam is resting on an elastic foundation. Forced vibration of FG-CNTRC beams with four different FG distribution patterns of reinforcement was studied by Ansari *et al.* (2014) through using Timoshenko beam theory and von Kármán geometric nonlinearity and employing generalized differential quadrature (GDQ) method to discretize the nonlinear governing equations. Wu *et al.* (2016) considered a geometrically imperfect FG-CNTRC beam and applied first-order shear deformation beam theory to study the nonlinear vibration. The governing equations were derived by utilizing the Ritz method and then solved by an iteration procedure. Recently, Ghorbani Shenasi *et al.* (2017) dealt with free vibration analysis of pre-twisted FG-CNTRC beams in thermal environment. They found that an increase in the pre-twist angle enhances the fundamental frequency parameters.

Meanwhile, analytical solutions are always needed for verification of numerical solutions to provide fast and accurate results for practical problems, whenever possible (Sedighi *et al.* 2012, Yazdi 2013, Javanmard *et al.* 2013, Bayat *et al.* 2013, Setoodeh and Afrahim 2014, Setoodeh *et al.* 2016, Setoodeh and Rezaei 2017a, b, Bağdatli 2015b, Togun and Bağdatli 2016b). According to the available literature and despite the attention given to CNTRCs, no analytical expressions for the nonlinear frequencies and post-buckling loads of FG-CNTRC beams have been derived so far. Accordingly, this paper aims to provide an analytical solution for nonlinear vibration and post-buckling behavior of Euler-Bernoulli nanocomposite beams reinforced by SWCNTs resting on a nonlinear elastic foundation. The governing equation is formulated via using Hamilton's principle and Galerkin's procedure. The variational iteration method is employed to solve the developed governing equation with quadratic and cubic nonlinearities and the analytical expressions are obtained for nonlinear natural frequencies, post-buckling loads and vibration response of the CNTRC beam. The influences of different parameters such as nanotube volume fraction, vibration amplitude, end supports, slenderness ratio and nonlinear foundation parameters on the natural frequencies and buckling loads of the CNTRC beams are illustrated through tables and figures.

## 2. Material properties of FG-CNTRC beam

It is assumed that the CNTRC beam is made of a mixture of SWCNTs as reinforcements and isotropic matrix. The distribution patterns of reinforcements in the thickness direction of the beam are shown in Fig. 1. The effective Young's modulus and shear modulus of CNTRC are predicted based on the rule of mixture and can be written as (Yas and Samadi 2012)

$$E_{11} = \eta_1 V^{cnt} E_{11}^{cnt} + V_m E_m \quad (1a)$$

$$\frac{\eta_2}{E_{22}} = \frac{V^{cnt}}{E_{22}^{cnt}} + \frac{V_m}{E_m} \quad (1b)$$

$$\frac{\eta_3}{G_{12}} = \frac{V^{cnt}}{G_{12}^{cnt}} + \frac{V_m}{G_m} \quad (1c)$$

where superscript and subscript *cnt* and *m* denote the material properties of CNTs and matrix, respectively.  $E_{11}^{cnt}$ ,  $E_{22}^{cnt}$  and  $G_{12}^{cnt}$  are respectively the Young's and shear moduli of SWCNTs;  $E_m$  and  $G_m$  are the corresponding material properties related to the isotropic matrix. Accounting for the size-dependent material properties,  $\eta_1$ ,  $\eta_2$  and  $\eta_3$  are CNTs efficiency parameters and can be evaluated through matching the elastic modulus of CNTRCs obtained from the rule of mixture with those from MD simulations (Han and Elliot 2007). Also,  $V^{cnt}$  and  $V_m$  refer respectively to the volume fractions of CNTs and matrix, with the relation  $V^{cnt} + V_m = 1$ . Using a similar manner, the Poisson's ratio  $\nu$  and mass density  $\rho$  can be given by

$$\nu = V^{cnt} \nu^{cnt} + V_m \nu_m, \quad \rho = V^{cnt} \rho^{cnt} + V_m \rho_m \quad (2)$$

The distribution of CNTs along the thickness direction of the FG-CNTRC beam is expressed as

$$V^{cnt} = \left(1 + \frac{2z}{h}\right) V_{cnt}^* \quad (3)$$

where

$$V_{cnt}^* = \frac{\Lambda^{cnt}}{\Lambda^{cnt} + \left(\frac{\rho^{cnt}}{\rho_m}\right)(1 - \Lambda^{cnt})} \quad (4)$$

where  $\Lambda^{cnt}$  is the mass fraction of the CNTs. It is noted that  $V^{cnt} = V_{cnt}^*$  corresponds to the FG-CNTRC beams with uniformly distribution of reinforcing phase.

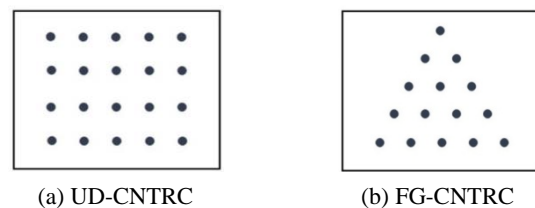


Fig. 1 SWCNTs distribution patterns in the FG-CNTRC beam

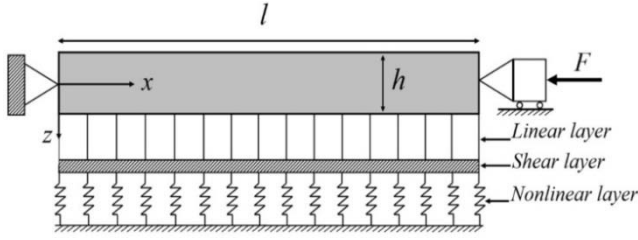


Fig. 2 Geometry of the FG-CNTRC beam on nonlinear elastic foundation

### 3. Governing equation

A CNTRC beam of length  $l$ , width  $b$  and thickness  $h$  resting on a nonlinear elastic foundation, and subjected to an axial force is shown in Fig. 2. Based on the Euler-Bernoulli beam theory, the displacements of an arbitrary point in the beam along the  $x$  and  $z$  axes can be described in the following form (Lai *et al.* 2012)

$$\tilde{U}(x, z, t) = U(x, t) - z \frac{\partial W(x, t)}{\partial x}, \quad \tilde{W}(x, z, t) = W(x, t) \quad (5)$$

where  $t$  denotes the time and  $U$  and  $W$  are, respectively, the axial and transverse displacements at the mid-surface of the beam with  $z = 0$ . The normal stress  $\sigma_{xx}$  takes the following form by utilizing the von Kármán strain-displacement relation and linear elastic constitutive law

$$\sigma_{xx} = Q_{11}(z) \left[ \frac{\partial U}{\partial x} - z \frac{\partial^2 W}{\partial x^2} + \frac{1}{2} \left( \frac{\partial W}{\partial x} \right)^2 \right] \quad (6)$$

where

$$Q_{11} = \frac{E_{11}(z)}{1 - \nu^2(z)} \quad (7)$$

According to Hamilton's principle, one can write

$$\int_0^t \delta(U_e - T - W_{ext}) dt = 0 \quad (8)$$

where  $\delta$  represents the variational symbol and  $U_e$ ,  $T$  and  $W_{ext}$  are respectively the strain energy, kinetic energy and work done by the external forces obtained as follows

$$U_e = \frac{b}{2} \int_0^l \int_{-h/2}^{h/2} Q_{11}(z) \left( \frac{\partial U}{\partial x} - z \frac{\partial^2 W}{\partial x^2} + \frac{1}{2} \left( \frac{\partial W}{\partial x} \right)^2 \right)^2 dz dx \quad (9)$$

$$T = \frac{b}{2} \int_0^l \int_{-h/2}^{h/2} \rho(z) \left[ \left( \frac{\partial U}{\partial t} \right)^2 + \left( \frac{\partial W}{\partial t} \right)^2 \right] dz dx \quad (10)$$

$$W_{ext} = \frac{b}{2} \int_0^l F \left( \frac{\partial W}{\partial x} \right)^2 dx - \frac{b}{2} \int_0^l \left[ k_l W^2 + \frac{1}{2} k_{nl} W^4 + k_s \left( \frac{\partial W}{\partial x} \right)^2 \right] dx \quad (11)$$

where  $F$  is the axial force and  $k_l$ ,  $k_{nl}$  and  $k_s$  are the linear,

nonlinear and shear coefficients of the nonlinear elastic foundation, respectively. Substituting Eqs. (9)-(11) into Hamilton's principle in Eq. (8) and applying integration by parts and then setting the coefficients of  $\delta U$  and  $\delta W$  equal to zero, yields

$$\delta U : \frac{\partial N}{\partial x} = I_1 \frac{\partial^2 U}{\partial t^2} \quad (12)$$

$$\delta W : \frac{\partial^2 M}{\partial x^2} + \frac{\partial}{\partial x} \left( N \frac{\partial W}{\partial x} \right) - k_l W - k_{nl} W^3 + (k_s - F) \frac{\partial^2 W}{\partial x^2} = I_1 \frac{\partial^2 W}{\partial t^2} \quad (13)$$

Also, the corresponding boundary conditions at end points are obtained as

$$U = 0 \quad \text{or} \quad N = 0 \quad (14)$$

$$\frac{\partial M}{\partial x} + (k_s + N - F) \frac{\partial W}{\partial x} = 0 \quad \text{or} \quad W = 0 \quad (15)$$

$$\frac{\partial W}{\partial x} = 0 \quad \text{or} \quad M = 0 \quad (16)$$

In Eqs. (12)-(13),  $M$  and  $N$  are respectively the bending moment and normal force stress resultants expressed as

$$N = A_{11} \left[ \frac{\partial U}{\partial x} + \frac{1}{2} \left( \frac{\partial W}{\partial x} \right)^2 \right] - B_{11} \frac{\partial^2 W}{\partial x^2} \quad (17)$$

$$M = B_{11} \left[ \frac{\partial U}{\partial x} + \frac{1}{2} \left( \frac{\partial W}{\partial x} \right)^2 \right] - D_{11} \frac{\partial^2 W}{\partial x^2} \quad (18)$$

where

$$\{A_{11}, B_{11}, D_{11}\} = \int_{-h/2}^{h/2} Q_{11}(z) \{1, z, z^2\} dz, \quad I_1 = \int_{-h/2}^{h/2} \rho(z) dz \quad (19)$$

Since the value of the longitudinal inertia is very small, then Eq. (12) can be simplified as  $N = \text{constant} = N_0$ . By integrating Eq. (17) with respect to  $x$  and considering  $U = 0$  at  $x = 0$  and  $x = l$ , i.e., immovable end supports

$$N_0 = \frac{A_{11}}{l} \int_0^l \left[ \frac{1}{2} \left( \frac{\partial W}{\partial x} \right)^2 - \frac{B_{11}}{A_{11}} \frac{\partial^2 W}{\partial x^2} \right] dx \quad (20)$$

In view of Eqs. (18) and (20), the bending moment is restated as

$$M = \frac{B_{11}}{A_{11}} \left[ N_0 + B_{11} \frac{\partial^2 W}{\partial x^2} \right] - D_{11} \frac{\partial^2 W}{\partial x^2} \quad (21)$$

By inserting Eq. (20) into (21) and then substituting the result into Eq. (13), the nonlinear governing equation of motion of the FG-CNTRC beam takes the following form

Table 1 Vibration modes of the CNTRC beam

Boundary condition	Mode shape $\phi(\zeta)$	Coefficient $\beta$
S-S	$C_n \sin(\beta_n \zeta)$	$\beta_1 = \pi \quad \beta_2 = 2\pi \quad \beta_3 = 3\pi$
C-C	$D_n \left[ \cosh(\beta_n \zeta) - \cos(\beta_n \zeta) - \frac{\cosh(\beta_n) - \cos(\beta_n)}{\sinh(\beta_n) - \sin(\beta_n)} (\sinh(\beta_n \zeta) - \sin(\beta_n \zeta)) \right]$	$\beta_1 = 4.7300 \quad \beta_2 = 7.8532$ $\beta_3 = 10.9956$
C-S	$Z_n \left[ \cosh(\beta_n \zeta) - \cos(\beta_n \zeta) - \frac{\cosh(\beta_n) - \cos(\beta_n)}{\sinh(\beta_n) - \sin(\beta_n)} (\sinh(\beta_n \zeta) - \sin(\beta_n \zeta)) \right]$	$\beta_1 = 3.9266 \quad \beta_2 = 7.0686$ $\beta_3 = 10.2102$

Table 2 Comparison of nonlinear frequency ratio ( $\omega_{nl}/\omega_l$ ) for S-S and C-C isotropic beams ( $l/h = 15$ )

	$W_{max}/\sqrt{I/S}$	1 <sup>st</sup> approximation	2 <sup>nd</sup> approximation	3 <sup>rd</sup> approximation	Azrar <i>et al.</i> (1999)	Ke <i>et al.</i> (2010b)
S-S	0.5	1.0232	1.0231	1.0231	-	1.0231
	1	1.0897	1.0892	1.0892	1.0892	1.0892
	2	1.3229	1.3180	1.3178	1.3178	1.3178
	3	1.6394	1.6263	1.6257	1.6257	1.6257
C-C	0.5	1.0056	1.0056	1.0056	-	1.0056
	1	1.0222	1.0222	1.0222	1.0222	1.0222
	2	1.0862	1.0857	1.0857	1.0857	1.0857
	3	1.1852	1.1832	1.1831	1.1831	1.1831

$$\left( \frac{B_{11}^2}{A_{11}} - D_{11} \right) \frac{\partial^4 W}{\partial x^4} + (N_0 + k_s - F) \frac{\partial^2 W}{\partial x^2} - k_l W - k_{nl} W^3 = I_1 \frac{\partial^2 W}{\partial t^2} \quad (22)$$

For generality and simplicity, the following dimensionless parameters are considered

$$\zeta = \frac{x}{l}, \quad (\bar{u}, \bar{w}) = \frac{(U, W)}{h}, \quad \eta = \frac{h}{l}, \quad \bar{I} = \frac{I_1}{I_{110}}, \quad (23)$$

$$\tau = \frac{t}{l} \sqrt{\frac{A_{110}}{I_{110}}}, \quad (a_{11}, b_{11}, d_{11}) = \left( \frac{A_{11}}{A_{110}}, \frac{B_{11}}{A_{110}h}, \frac{D_{11}}{A_{110}h^2} \right)$$

where  $A_{110}$  and  $I_{110}$  are the corresponding values of  $A_{11}$  and  $I_1$  for a homogenous beam made of matrix material. Using above dimensionless quantities leads to the following dimensionless governing equation

$$d_0 \eta^2 \frac{\partial^4 \bar{w}}{\partial \zeta^4} + (\bar{N}_0 + K_s - \bar{F}) \frac{\partial^2 \bar{w}}{\partial \zeta^2} - K_l \bar{w} - K_{nl} \bar{w}^3 = \bar{I} \frac{\partial^2 \bar{w}}{\partial \tau^2} \quad (24)$$

where  $K_l$ ,  $K_{nl}$  and  $K_s$  are the dimensionless coefficients of the nonlinear elastic foundation and  $\bar{F}$  is the dimensionless axial force defined as

$$K_l = \frac{l^2 k_l}{A_{110}}, \quad K_{nl} = \frac{l^2 h^2 k_{nl}}{A_{110}}, \quad K_s = \frac{k_s}{A_{110}}, \quad \bar{F} = \frac{F}{A_{110}} \quad (25)$$

Also

$$\bar{N}_0 = a_{11} \eta^2 \int_0^1 \left[ \frac{1}{2} \left( \frac{\partial \bar{w}}{\partial \zeta} \right)^2 - \frac{b_{11}}{a_{11}} \frac{\partial^2 \bar{w}}{\partial \zeta^2} \right] d\zeta, \quad d_0 = \frac{b_{11}^2}{a_{11}} - d_{11} \quad (26)$$

Separation of variable analysis and Galerkin method are employed to obtain the uncoupled nonlinear ordinary differential equation. The transverse displacement equation of the beam can be written as multiplication of two independent functions

$$\bar{w}(\zeta, \tau) = \phi(\zeta) w(\tau) \quad (27)$$

where  $\phi$  is the fundamental vibration mode of the beam which must satisfy the kinematic boundary conditions and is presented in Table 1 (Rao 2007). The values of  $C_n$ ,  $D_n$  and  $Z_n$  are obtained according to the maximum displacements of the beam, which are computed as  $C_1 = 1$ ,  $D_1 = 0.6297$  and  $Z_1 = 0.6626$  for the first mode. Also,  $w$  is an unknown time-dependent function which should be determined. Employing Galerkin's procedure, the governing equation takes the following simplified form

$$\ddot{w} + (\gamma_1 + \alpha_1 + \alpha_2 + \bar{F} \alpha_f) w + \gamma_2 w^2 + (\gamma_3 + \alpha_3) w^3 = 0 \quad (28)$$

where

$$\gamma_1 = \frac{-d_0 \eta^2 \int_0^1 \frac{d^4 \phi}{d\zeta^4} \phi d\zeta}{\lambda_0}, \quad \alpha_1 = \frac{K_l \int_0^1 \phi^2 d\zeta}{\lambda_0}, \quad (29)$$

$$\gamma_2 = \frac{b_{11} \eta^2 \int_0^1 \frac{d^2 \phi}{d\zeta^2} d\zeta \int_0^1 \frac{d^2 \phi}{d\zeta^2} \phi d\zeta}{\lambda_0}$$

$$\gamma_3 = \frac{-a_{11}\eta^2 \int_0^1 \left(\frac{d\phi}{d\zeta}\right)^2 d\zeta \int_0^1 \frac{d^2\phi}{d\zeta^2} \phi d\zeta}{2\lambda_0}$$

$$\alpha_2 = \frac{-K_s \int_0^1 \frac{d^2\phi}{d\zeta^2} \phi d\zeta}{\lambda_0}, \quad \alpha_3 = \frac{K_{nl} \int_0^1 \phi^4 d\zeta}{\lambda_0} \quad (29)$$

$$\alpha_F = \frac{\int_0^1 \frac{d^2\phi}{d\zeta^2} \phi d\zeta}{\lambda_0}, \quad \lambda_0 = \bar{I} \int_0^1 \phi^2 d\zeta$$

Three types of end supports are considered for the FG-CNTRC beams, simply supported at both ends (S-S), clamped at both ends (C-C) and clamped at  $x = 0$  and simply supported at  $x = l$  (C-S). For each of them, the following boundary conditions must be satisfied:

- Simply supported-simply supported

$$\phi(0) = \phi(1) = 0, \quad \frac{d^2\phi(0)}{d\zeta^2} = \frac{d^2\phi(1)}{d\zeta^2} = 0 \quad (30)$$

- Clamped-clamped

$$\phi(0) = \phi(1) = 0, \quad \frac{d\phi(0)}{d\zeta} = \frac{d\phi(1)}{d\zeta} = 0 \quad (31)$$

- Clamped-simply supported

$$\phi(0) = \phi(1) = 0, \quad \frac{d\phi(0)}{d\zeta} = \frac{d^2\phi(1)}{d\zeta^2} = 0 \quad (32)$$

The initial conditions for vibration of CNTRC beams are

$$w(0) = \bar{w}_{\max}, \quad \frac{dw(0)}{d\tau} = 0 \quad (33)$$

In the post-buckling analysis, the variation with respect to time is zero. Therefore, according to Eq. (28), the post-buckling load of the FG-CNTRC beams can be obtained as

$$\bar{F} = F_{nl} = -\frac{(\gamma_1 + \alpha_1 + \alpha_2) + \gamma_2 a + (\gamma_3 + \alpha_3) a^2}{\alpha_F} \quad (34)$$

where  $a$  is the maximum dimensionless deflection of the beam at  $t = 0$ , i.e.,  $a = \bar{w}_{\max}$ . By neglecting nonlinear and time dependent terms in Eq. (28), the critical buckling load can be also determined as

$$F_l = -\frac{\gamma_1 + \alpha_1 + \alpha_2}{\alpha_F} \quad (35)$$

#### 4. Method of solution

There are several classical methods for solving nonlinear differential equations. But, due to the difficulties and limitations associated with analytical solutions,

different numerical techniques have become more popular in recent years. The variational iteration method is an analytical method presented by He (1999), which has overcome the difficulties of traditional perturbation/non-perturbation techniques and has many advantages such as fast convergence and ease of calculations along with the accuracy. Furthermore, this method provides closed form solutions which are really important for parametric studies.

In VIM, a general differential equation can be stated in the following form (He 2007)

$$Lu(t) + \Gamma u(t) = g(t) \quad (36)$$

where  $L$ ,  $\Gamma$  and  $g(t)$  are, respectively, linear operator, nonlinear operator and a real inhomogeneous term. The main concept of this method is to find a correction functional as follows

$$u_{n+1}(t) = u_n(t) + \int_0^t \lambda (Lu_n(s) + \Gamma \tilde{u}_n(s) - g(s)) ds \quad (37)$$

in which  $\lambda$  is the general Lagrange multiplier that can be determined using the stationary conditions of variational theory. The subscript  $n$  refers to  $n$ th order approximation, and  $\tilde{u}_n$  denotes a restricted variation, i.e.,  $\delta \tilde{u}_n = 0$ .

#### 4.1 Application of VIM to vibration analysis

By omitting the axial force in Eq. (28) and defining the following coefficients for simplicity, one obtains

$$\ddot{w}(\tau) + \theta_1 w(\tau) + \theta_2 w^2(\tau) + \theta_3 w^3(\tau) = 0 \quad (38)$$

$$\theta_1 = \gamma_1 + \alpha_1 + \alpha_2, \quad \theta_2 = \gamma_2, \quad \theta_3 = \gamma_3 + \alpha_3$$

Now by introducing  $f$  as a function of  $w$ , Eq. (38) can be rewritten as

$$\ddot{w} + \omega^2 w + f(w) = 0 \quad (39)$$

$$f(w) = \theta_1 w + \theta_2 w^2 + \theta_3 w^3 - \omega^2 w$$

In which,  $\omega$  is the dimensionless natural frequency defined according to Eq. (40) in terms of the natural frequency  $\bar{\omega}$  as

$$\omega = \bar{\omega} l \sqrt{\frac{I_{110}}{A_{110}}} \quad (40)$$

Substituting Eq. (39) into Eq. (37), and calculating the variation with respect to  $w$  and using integration by parts leads to the following equation

$$\delta w_{n+1}(\tau) = \delta w_n(\tau) + \left( \lambda(s) \delta \frac{dw_n(s)}{ds} \right) \Big|_{s=\tau}$$

$$- \left( \frac{d\lambda(s)}{ds} \delta w_n(s) \right) \Big|_{s=\tau} + \int_0^\tau \left[ \left( \frac{d^2\lambda(s)}{ds^2} + \omega^2 \lambda(s) \right) \delta w_n(s) \right] ds \quad (41)$$

Therefore, the Lagrange multiplier must satisfy the following stationary conditions

Table 3 Nonlinear frequency ratio ( $\omega_{nl}/\omega_l$ ) for S-S ( $E_2/E_1 = 5$ ) and C-S ( $E_2/E_1 = 0.2$ ) beams ( $l/h = 16$ )

$W_{\max}/\sqrt{I/S}$	S-S		C-S	
	Present	Lai <i>et al.</i> (2012)	Present	Lai <i>et al.</i> (2012)
1	1.0789	1.0787	1.0479	1.0476
2	1.3320	1.3293	1.1776	1.1772
3	1.6713	1.6622	1.3669	1.3673
4	2.0397	2.0261	1.5965	1.5984

$$\left( \frac{d^2\lambda(s)}{ds^2} + \omega^2\lambda(s) \right) \Big|_{s=\tau} = 0 \quad (42)$$

$$1 - \frac{d\lambda(s)}{ds} \Big|_{s=\tau} = 0, \quad \lambda(s=\tau) = 0$$

Accordingly, the Lagrange multiplier can be determined as

$$\lambda(s) = \frac{1}{\omega} \sin(\omega(s-\tau)) \quad (43)$$

Considering the initial conditions in Eq. (33) and based on the response of linear vibration of the beam, for the first iteration,  $w_0$  is estimated as

$$w_0 = a \cos(\omega\tau) \quad (44)$$

Therefore, the first-order approximation is obtained as

$$w_1 = a \cos(\omega\tau) + \int_0^\tau \frac{1}{\omega} \sin(\omega(s-\tau)) \left( -a\omega^2 + a\theta_1 + \frac{3}{4}\theta_3 a^3 \right) \cos(\omega s) + \frac{1}{4}\theta_3 a^3 \cos(3\omega s) + \frac{1}{2}\theta_2 a^2 \cos(2\omega s) + \frac{1}{2}\theta_2 a^2 ds \quad (45)$$

The coefficient of the  $\cos(\omega s)$  must be equal to zero to avoid producing secular terms in the next iterations, thus

$$\omega_0 = \sqrt{\theta_1 + \frac{3}{4}\theta_3 a^2} \quad (46)$$

where  $\omega_0$  is the first-order approximation of the natural

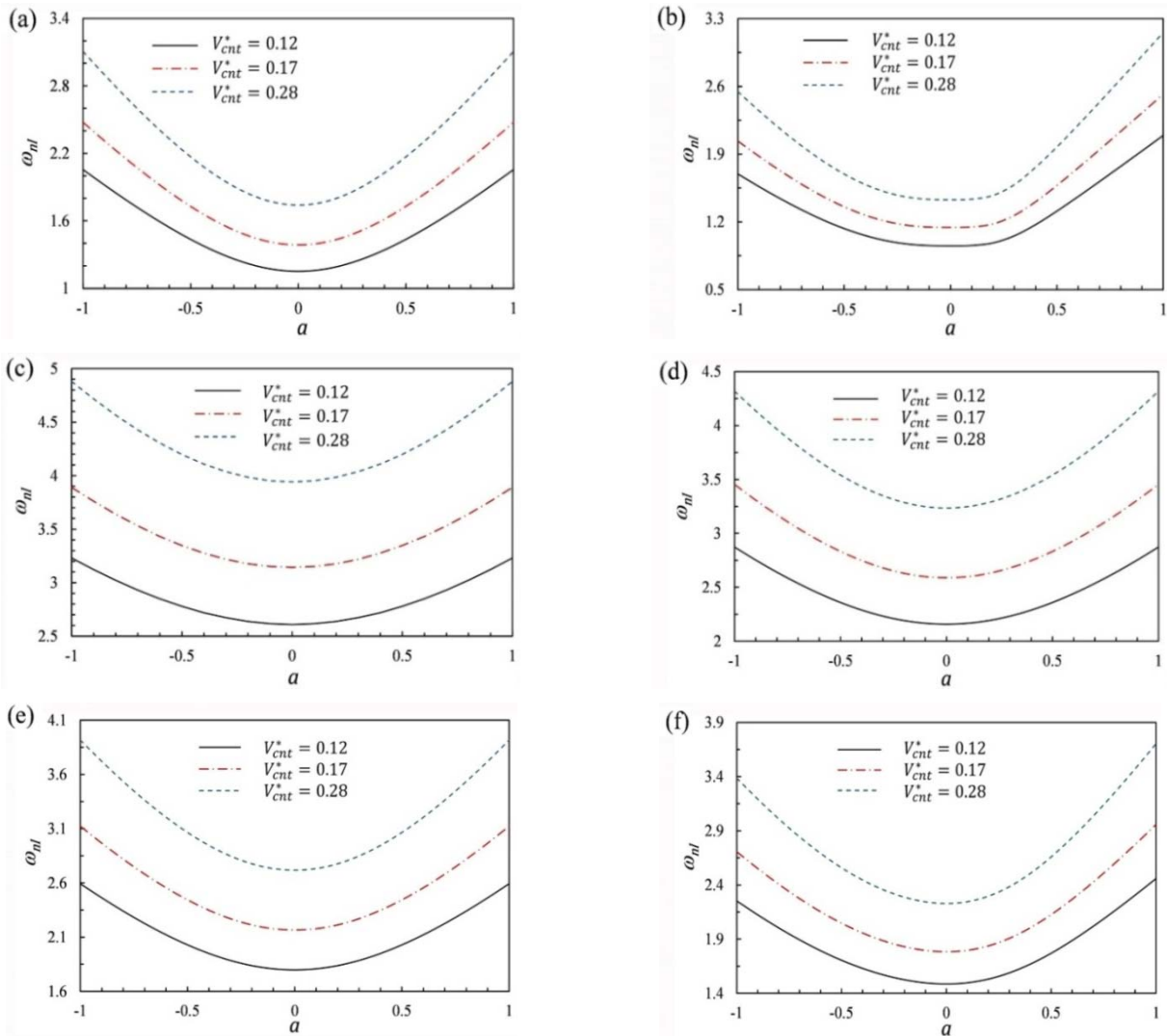


Fig. 3 Dimensionless nonlinear frequencies versus vibration amplitude for CNTRC beams with different volume fractions: (a) S-S UD; (b) S-S FG; (c) C-C UD; (d) C-C FG; (e) C-S UD; and (f) C-S FG

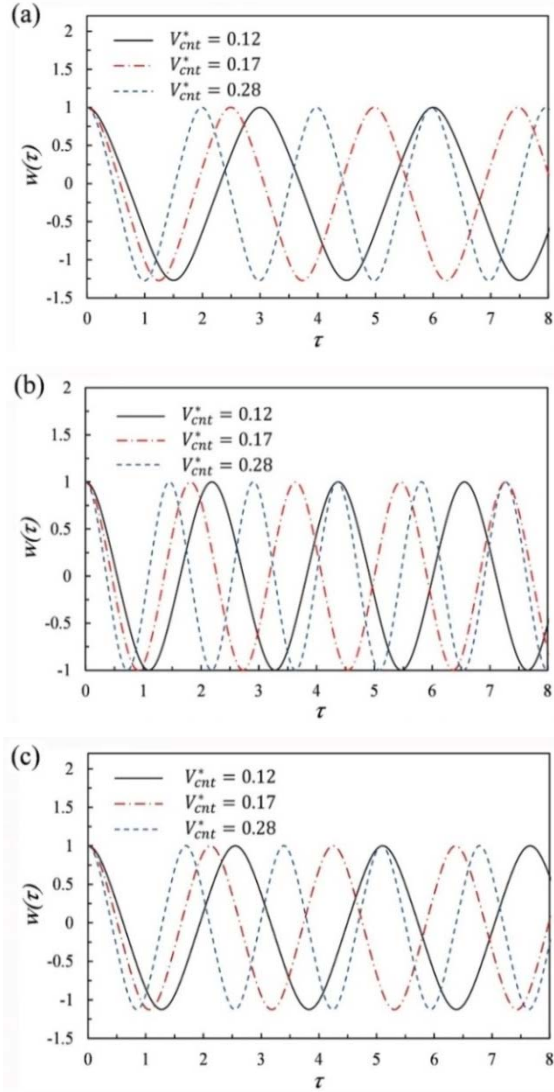


Fig. 4 Vibration response of FG-CNTRC beams at  $a = 1$ : (a) S-S; (b) C-C; and (c) C-S

nonlinear frequency. It is worth noting that in the case of linear vibration, the linear natural frequency can be obtained as  $\omega_l = \sqrt{\theta_1}$ . Also, the first-order approximate solution for  $w$  is developed as

$$w_1 = A_1 \cos(\omega\tau) + A_2 \cos(2\omega\tau) + A_3 \cos(3\omega\tau) + A_4 \quad (47)$$

where

$$A_1 = a + \frac{\theta_2 a^2}{3\omega^2} - \frac{\theta_3 a^3}{32\omega^2}, \quad A_2 = \frac{\theta_2 a^2}{6\omega^2}, \quad (48)$$

$$A_3 = \frac{\theta_3 a^3}{32\omega^2}, \quad A_4 = -\frac{\theta_2 a^2}{2\omega^2}$$

By repeating the previous procedure and avoiding the secular terms, the natural frequency and periodic solution of the second-order approximation can be determined which are given in Appendix A. The third-order approximation can be also calculated similarly. However, the formulations are not brought here for the sake of brevity and only the related

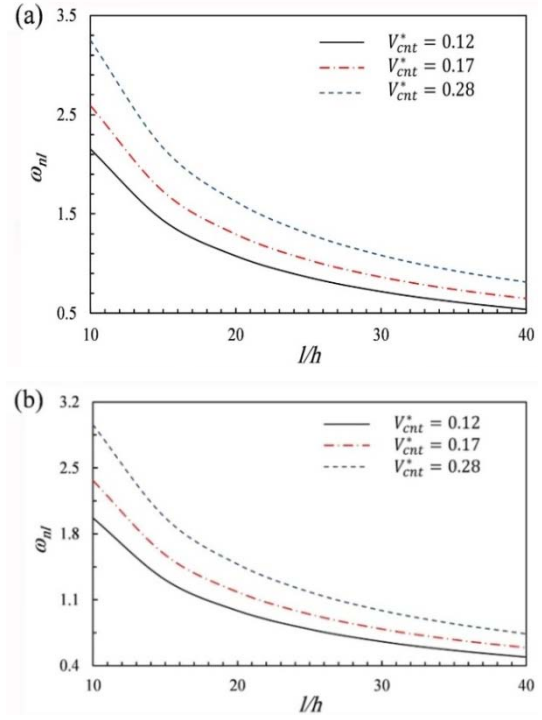


Fig. 5 Dimensionless nonlinear frequencies versus slenderness ratio for S-S CNTRC beams at  $a = 0.5$ : (a) UD; and (b) FG

results are exhibited to demonstrate the fast convergence of the method.

## 5. Results and discussions

At the first stage, the fast convergence and accuracy of the solution are verified. The results of first, second and third iterations for the nonlinear frequency ratios ( $\omega_{nl}/\omega_l$ ) of isotropic homogenous S-S and C-C beams at different vibration amplitudes ( $W_{\max}/\sqrt{I/S}$ ) are presented in Table 2. Note that  $W_{\max}$  is the dimensional maximum transverse displacement,  $I$  denotes the area moment of inertia and  $S$  is the cross-section area of the beam. It is found that the present results exhibit excellent agreement with those available solutions reported by other references used direct numerical integration method (Ke *et al.* 2010b) and harmonic balance method (Azrar *et al.* 1999). Moreover, the fast rate of convergence of the results is observed. Table 3 shows a comparison between the predicted values of the nonlinear frequency ratios ( $\omega_{nl}/\omega_l$ ) and those reported by Lai *et al.* (2012) based on an analytical perturbation approach for large amplitude vibration of functionally graded beams. The nonlinear frequency ratios at different vibration amplitudes for both of simply supported-simply supported and clamped-simply supported FG beams with materials properties of  $E_1 = 70$  GPa,  $\nu_1 = 0.33$  and  $\rho_1 = 2780$  kg/m<sup>3</sup> are presented. The subscripts 1 and 2 denote the top surface and the bottom surface of the FG beam, respectively. Again, a good agreement between the solutions is achieved.

At the second part, some parametric studies are performed to show the effects of different parameters on the

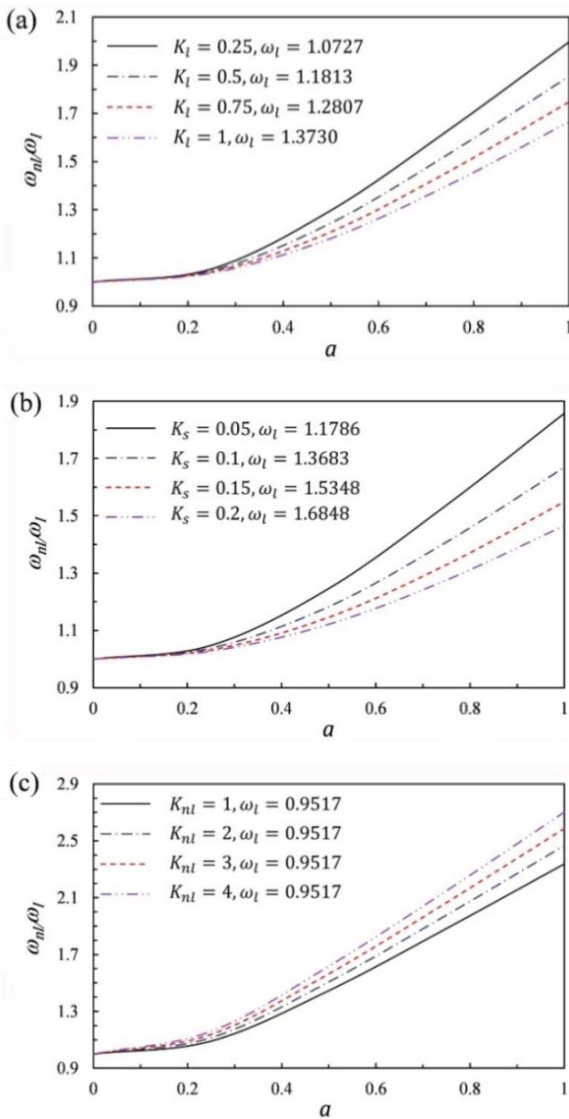


Fig. 6 Nonlinear frequency ratios versus vibration amplitude of S-S FG-CNTRC beams with  $V_{cnt}^* = 0.12$  for different values of foundation parameters: (a)  $K_I$  ( $K_S = K_{nl} = 0$ ); (b)  $K_S$  ( $K_I = K_{nl} = 0$ ); and (c)  $K_{nl}$  ( $K_I = K_S = 0$ )

vibration and stability behavior of FG-CNTRC beams. Both of the uniform and functionally graded distributions of nanotubes are considered which are designated respectively by UD-CNTRC and FG-CNTRC. The selected matrix material is Poly methyl methacrylate (PMMA) with  $\nu_m = 0.3$ ,  $\rho_m = 1190 \text{ kg/m}^3$  and  $E_m = 2.5 \text{ GPa}$  at room temperature. The armchair (10, 10) SWCNTs are considered as reinforcements with  $\nu^{cnt} = 0.19$ ,  $E_{11}^{cnt} = 600 \text{ GPa}$  and  $\rho^{cnt} = 1400 \text{ kg/m}^3$ . By modifying the rule of mixture based on molecular dynamics results, the CNT efficiency parameters  $\eta_j$  ( $j = 1, 2, 3$ ) are introduced according to the reported effective properties of CNTRCs. The efficiency parameters are obtained by matching the atomistic values of Young's moduli with the counterparts computed by the modified form of the rule of mixture as (Yas and Samadi 2012):  $\eta_1 = 1.2833$ ,  $\eta_2 = 1.0556$  for  $V_{cnt}^* = 0.12$ ;  $\eta_1 = 1.3414$ ,  $\eta_2 = 1.7101$  for  $V_{cnt}^* = 0.17$ ;  $\eta_1 = 1.3238$ ,  $\eta_2 = 1.7380$  for  $V_{cnt}^* =$

0.28. Also, it is assumed that  $\eta_2 = \eta_3$ . For PMMA/CNT composites, the beams have slenderness ratio of  $l/h = 15$ , unless otherwise stated.

Fig. 3 shows the variations of dimensionless nonlinear frequency versus dimensionless vibration amplitude for UD- and FG-CNTRC beams with different boundary Conditions.

It is found that for S-S and C-S FG-CNTRC beams, the curves are unsymmetrical which is due to presence of quadratic nonlinearity in the governing equation that refers to bending-stretching coupling effect. Also, it can be observed that increase in the vibration amplitude and CNT volume fraction leads to the higher nonlinear frequencies. It can be seen that for both distributions with increasing the constraints at the edges of the beams, the nonlinear frequency ratio decreases. Furthermore, the degree of hardening type of nonlinearity is less for the C-C boundary condition compared to those of C-S and S-S boundary conditions. Fig. 4 depicts the vibration response of S-S, C-C and C-S FG-CNTRC beams versus dimensionless time in terms of different volume fractions. It is shown that the S-S and C-S beams oscillate unsymmetrically which is related to the bending-stretching coupling effect. Fig. 5 demonstrates the effect of slenderness ratio on the dimensionless nonlinear frequencies of S-S CNTRC beams with different volume fractions. It can be concluded that the natural frequency decreases with increasing the slenderness ratio. Furthermore, the impact of nonlinear elastic foundation coefficients on the dimensionless nonlinear frequency ratio of S-S FG-CNTRC beams is investigated in Fig. 6. It can be noticed that an increase in the nonlinear elastic foundation coefficient leads to larger nonlinear frequency ratio. Moreover, the beams with the smallest linear and shear foundation coefficients possess the highest nonlinear frequency ratios.

The variations of dimensionless post-buckling loads versus dimensionless maximum deflection for S-S, C-C and C-S CNTRC beams having different volume fractions are demonstrated in Fig. 7. The results reveal that increase in both the maximum deflection of the beam and volume fraction enhances the post-buckling load of the CNTRC beams. Moreover, as expected, the values of post-buckling loads of C-C beams are larger than those of C-S and S-S beams. In Fig. 8, the dimensionless post-buckling loads of beams with different volume fractions versus slenderness ratio are plotted. One can see that the post-buckling load decreases with increasing the slenderness ratio. Additionally, the influences of nonlinear elastic foundation parameters on the dimensionless post-buckling load ratio ( $F_{nl}/F_l$ ) of beams with simply supported boundary conditions are studied in Fig. 9. As observed, an enhance in the linear and shear coefficients of the elastic foundation results in smaller dimensionless post-buckling load ratio. However, it is noticeable that the value of the dimensionless post-buckling load ratio increases with increasing the nonlinear elastic foundation parameter. It can be also seen that the nonlinearity is more significant for larger values of foundation stiffness and the effect of nonlinearity is enhanced with increasing the elastic foundation coefficients.

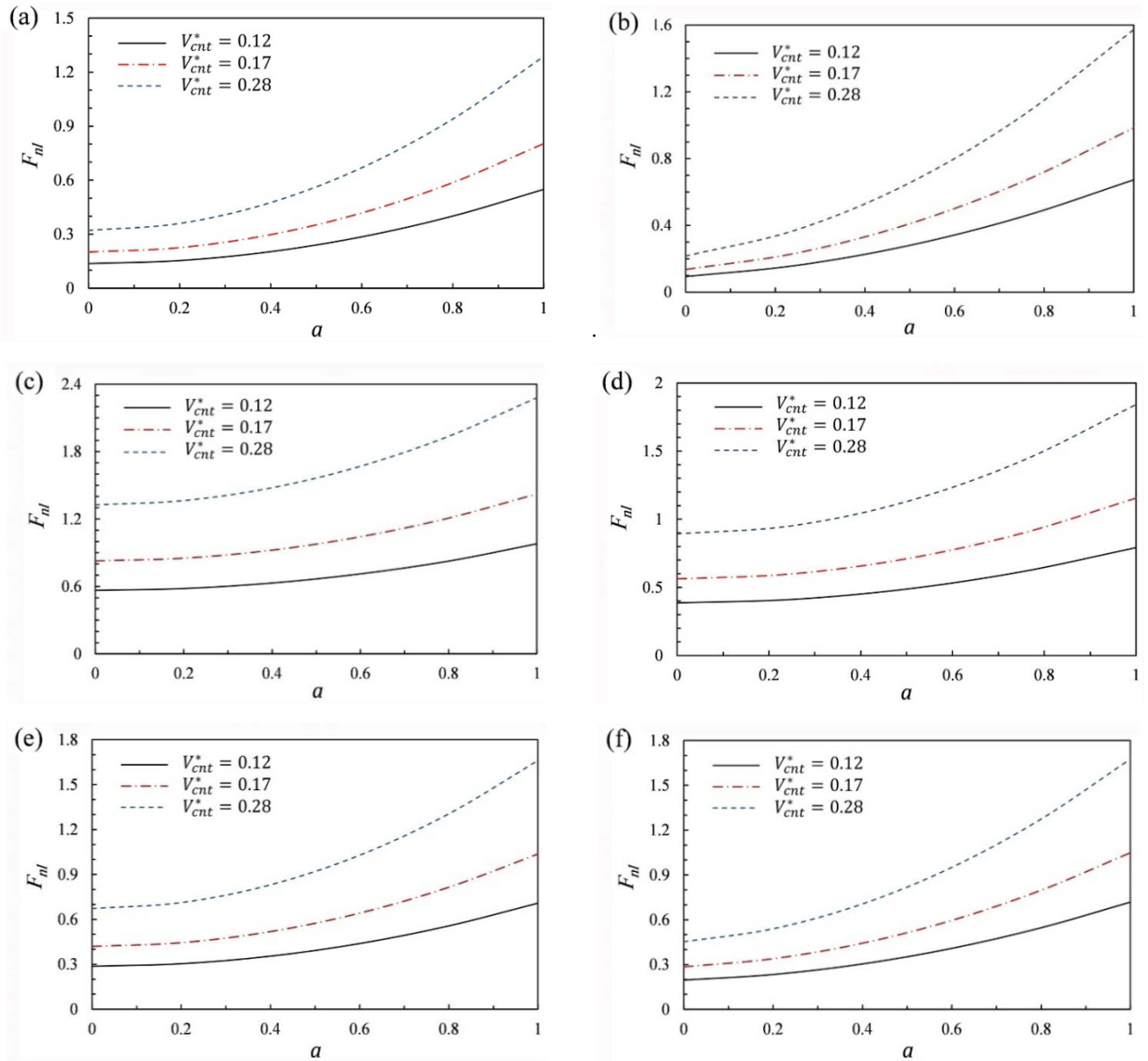


Fig. 7 Dimensionless post-buckling loads versus dimensionless maximum deflection of CNTRC beams with different volume fractions: (a) S-S UD; (b) S-S FG; (c) C-C UD; (d) C-C FG; (e) C-S UD; and (f) C-S FG

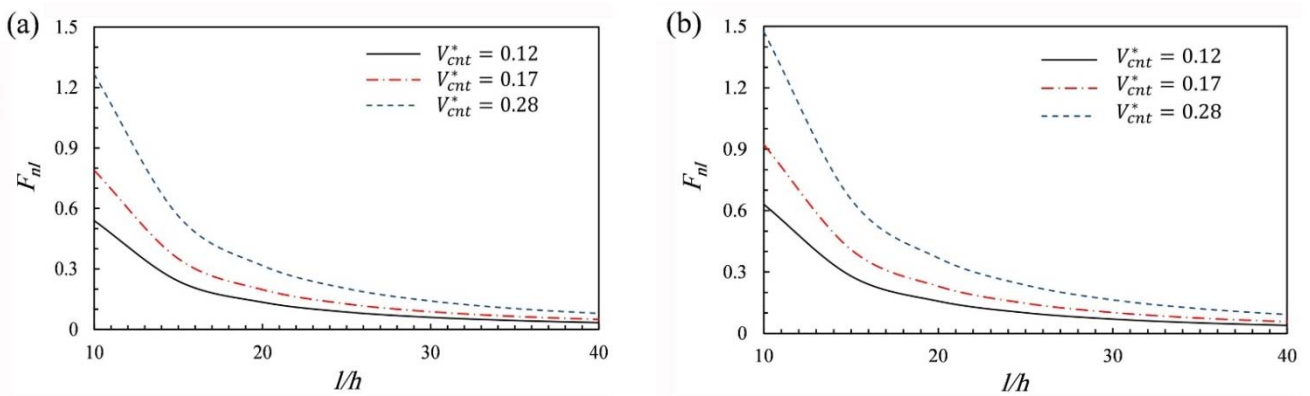


Fig. 8 Dimensionless post-buckling loads versus slenderness ratio for S-S CNTRC beams at  $a = 0.5$ : (a) UD; and (b) FG

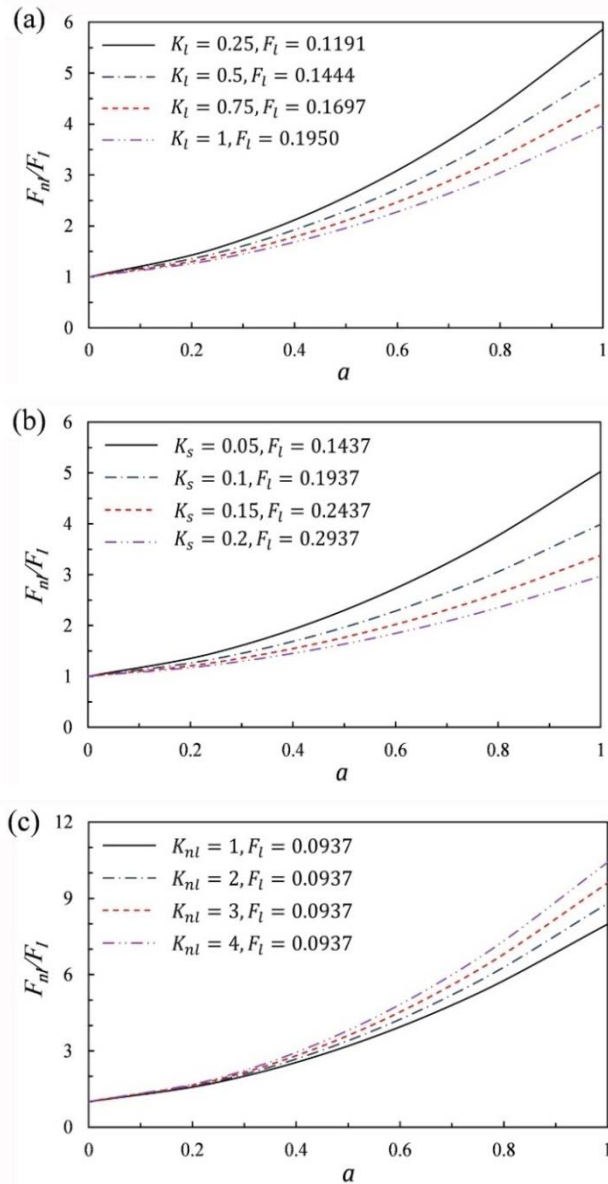


Fig. 9 Post-buckling load ratios versus dimensionless maximum deflection of S-S FG-CNTRC beams with  $V_{cnt}^* = 0.12$  for different values of foundation parameters: (a)  $K_l$  ( $K_s = K_{nl} = 0$ ); (b)  $K_s$  ( $K_l = K_{nl} = 0$ ); and (c)  $K_{nl}$  ( $K_l = K_s = 0$ )

## 6. Conclusions

As a first endeavor, the closed form solutions for nonlinear natural frequencies, vibration response and post-buckling loads of nanocomposite beams reinforced by single-walled carbon nanotubes are provided based on Euler-Bernoulli beam theory and von Kármán geometric nonlinearity. It is assumed that the beam is resting on a nonlinear elastic foundation to present a more general problem. The material properties of the CNTRC beams are graded through the thickness of the beam and the modified form of the rule of mixture is used to estimate the effective properties. Employing the variational iteration method, the nonlinear governing equations are analytically solved to present explicit relations for the vibration and stability

response of the nanocomposite beams. The correctness and fast convergence rate of the method are demonstrated through several examples that include isotropic and functionally graded beams with different combinations of simply supported and clamped boundary conditions. Moreover, the formulation provides the possibility of performing different parametric studies. Specifically, the influences of the CNTs distributions and volume fractions, maximum deflection of the beam, slenderness ratio, elastic foundation and boundary conditions on the nonlinear free vibration and post-buckling of FG-CNTRC beams are discussed. The results demonstrate the necessity of conducting a nonlinear analysis even for small values of the vibration amplitude. It is observed that the increase in the CNT volume fraction, vibration amplitude or maximum deflection results in increasing the nonlinear natural frequencies as well as post-buckling loads. Furthermore, the results reveal that the nonlinear frequency ratio of S-S and C-S beams is dependent on both the magnitude and sign of the vibration amplitude.

## References

- Alesadi, A., Galehdari, M. and Shojaee, S. (2017), "Free vibration and buckling analysis of cross-ply laminated composite plates using Carrera's unified formulation based on Isogeometric approach", *Comput. Struct.*, **183**, 38-47.
- Anjana, R., Sharma, S. and Bansal, A. (2016), "Molecular dynamics simulation of carbon nanotube reinforced polyethylene composites", *J. Compos. Mater.*  
DOI: 10.1177/0021998316674264
- Ansari, R., Faghieh Shojaei, M., Mohammadi, V., Gholami, R. and Sadeghi, F. (2014), "Nonlinear forced vibration analysis of functionally graded carbon nanotube-reinforced composite Timoshenko beams", *Compos. Struct.*, **113**, 316-327.
- Azrar, L., Benamar, R. and White, R.G. (1999), "A semi-analytical approach to the nonlinear dynamic response problem of S-S and C-C beams at large vibration amplitudes, part I: General theory and application to the single mode approach to free and forced vibration analysis", *J. Sound Vib.*, **224**(2), 183-207.
- Bağdatlı, S.M. (2015a), "Non-linear vibration of nanobeams with various boundary condition based on nonlocal elasticity theory", *Compos. Part B: Eng.*, **80**, 43-52.
- Bağdatlı, S.M. (2015b), "Non-linear transverse vibrations of tensioned nanobeams using nonlocal beam theory", *Struct. Eng. Mech., Int. J.*, **55**(2), 281-298.
- Bayat, M., Pakar, I. and Emadi, A. (2013), "Vibration of electrostatically actuated microbeam by means of homotopy perturbation method", *Struct. Eng. Mech., Int. J.*, **48**(6), 823-831.
- Biswal, M., Sahu, S.K. and Asha, A.V. (2016), "Vibration of composite cylindrical shallow shells subjected to hygrothermal loading-experimental and numerical results", *Compos. Part B: Eng.*, **98**, 108-119.
- Cadec, M., Coleman, J.N., Barron, V., Hedicke, K. and Blau, W.J. (2002), "Morphological and mechanical properties of carbon-nanotube-reinforced semicrystalline and amorphous polymer composites", *Appl. Phys. Lett.*, **81**(27), 5123-5125.
- Esawi, A.M.K. and Farag, M.M. (2007), "Carbon nanotube reinforced composites: potential and current challenges", *Mater. Des.*, **28**(9), 2394-2401.
- Fiedler, B., Gojny, F.H., Wichmann, M.H.G., Nottle, M.C.M. and Schulte, K. (2006), "Fundamental aspects of nano-reinforced composites", *Compos. Sci. Technol.*, **66**(16), 3115-3125.

- Formica, G., Lacarbonara, W. and Alessi, R. (2010), "Vibrations of carbon nanotube-reinforced composites", *J. Sound Vib.*, **329**(10), 1875-1889.
- Ghorbani Shenaa, A., Malekzadeh, P. and Ziaee, S. (2017), "Vibration analysis of pre-twisted functionally graded carbon nanotube reinforced composite beams in thermal environment", *Compos. Struct.*, **162**, 325-340.
- Han, Y. and Elliot, J. (2007), "Molecular dynamics simulations of the elastic properties of polymer/carbon nanotube composites", *Comput. Mater. Sci.*, **39**(2), 315-323.
- He, J.H. (1999), "Variational iteration method—a kind of non-linear analytical technique: some examples", *Int. J. Non-Linear Mech.*, **34**(4), 699-708.
- He, J.H. (2007), "Variational iteration method—Some recent results and new interpretations", *J. Comput. Appl. Math.*, **207**(1), 3-17.
- Heydarpour, Y., Aghdam, M.M. and Malekzadeh, P. (2014), "Free vibration analysis of rotating functionally graded carbon nanotube-reinforced composite truncated conical shells", *Compos. Struct.*, **117**, 187-200.
- Iijima, S. (1991), "Helical microtubules of graphitic carbon", *Nature*, **354**(6348), 56-58.
- Javanmard, M., Bayat, M. and Ardakani, A. (2013), "Nonlinear vibration of Euler-Bernoulli beams resting on linear elastic foundation", *Steel Compos. Struct., Int. J.*, **15**(4), 439-449.
- Jooybar, N., Malekzadeh, P. and Fiouz, A. (2016), "Vibration of functionally graded carbon nanotubes reinforced composite truncated conical panels with elastically restrained against rotation edges in thermal environment", *Compos. Part B: Eng.*, **106**, 242-261.
- Ke, L.L., Yang, J. and Kitipornchai, S. (2010a), "Nonlinear free vibration of functionally graded carbon nanotube-reinforced composite beams", *Compos. Struct.*, **92**(3), 676-683.
- Ke, L.L., Yang, J. and Kitipornchai, S. (2010b), "An analytical study on the nonlinear vibration of functionally graded beams", *Meccanica*, **45**(6), 743-752.
- Lai, S.K., Harrington, J., Xiang, Y. and Chow, K.W. (2012), "Accurate analytical perturbation approach for large amplitude vibration of functionally graded beams", *Int. J. Non-Linear Mech.*, **47**(5), 473-480.
- Lu, X.X. and Hu, Z. (2012), "Mechanical property evaluation of single-walled carbon nanotubes by finite element modeling", *Compos. Part B: Eng.*, **43**(4), 1902-1913.
- Malekzadeh, P. and Dehbozorgi, M. (2016), "Low velocity impact analysis of functionally graded carbon nanotubes reinforced composite skew plates", *Compos. Struct.*, **140**, 728-748.
- Malekzadeh, P. and Heydarpour, Y. (2015), "Mixed Navier-layerwise differential quadrature three-dimensional static and free vibration analysis of functionally graded carbon nanotube reinforced composite laminated plates", *Meccanica*, **50**(1), 143-167.
- Malekzadeh, P. and Setoodeh, A.R. (2007), "Large deformation analysis of moderately thick laminated plates on nonlinear elastic foundation by DQM", *Compos. Struct.*, **80**(4), 569-579.
- Malekzadeh, P. and Vosoughi, A.R. (2009), "DQM large amplitude vibration of composite beams on nonlinear elastic foundation with restrained edges", *Commun. Nonlinear Sci. Numer. Simul.*, **14**(3), 906-915.
- Malekzadeh, P. and Zarei, A.R. (2014), "Free vibration of quadrilateral laminated plates with carbon nanotube reinforced composite layers", *Thin-Wall. Struct.*, **82**, 221-232.
- Mehrabadi, S.J., Aragh, B.S., Khoshkharesh, V. and Taherpour, A. (2012), "Mechanical buckling of nanocomposite rectangular plate reinforced by aligned and straight single-walled carbon nanotubes", *Compos. Part B: Eng.*, **43**(4), 2031-2040.
- Rao, S.S. (2007), *Vibration of Continuous Systems*, John Wiley and Sons, Hoboken, NJ, USA.
- Sahoo, R. and Singh, B.N. (2014), "A new trigonometric zigzag theory for buckling and free vibration analysis of laminated composite and sandwich plates", *Compos. Struct.*, **117**, 316-332.
- Sedighi, H.M., Shirazi, K.H. and Zare, J. (2012), "An analytic solution of transversal oscillation of quintic non-linear beam with homotopy analysis method", *Int. J. Non-Linear Mech.*, **47**(7), 777-784.
- Setoodeh, A.R. and Afrahim, S. (2014), "Nonlinear dynamic analysis of FG micro-pipes conveying fluid based on strain gradient theory", *Compos. Struct.*, **116**, 128-135.
- Setoodeh, A.R. and Rezaei, M. (2017a), "Large amplitude free vibration analysis of functionally graded nano/micro beams on nonlinear elastic foundation", *Struct. Eng. Mech., Int. J.*, **61**(2), 209-220.
- Setoodeh, A.R. and Rezaei, M. (2017b), "An explicit solution for the size-dependent large amplitude transverse vibration of thin functionally graded micro-plates", *Sci. Iran*. [In press]
- Setoodeh, A.R. and Shojaee, M. (2016), "Application of TW-DQ method to nonlinear free vibration analysis of FG carbon nanotube-reinforced composite quadrilateral plates", *Thin-Wall. Struct.*, **108**, 1-11.
- Setoodeh, A.R. and Shojaee, M. (2017), "Critical buckling load optimization of functionally graded carbon-nanotube reinforced laminated composite quadrilateral plates", *Polym. Compos.* DOI: 10.1002/pc.24289
- Setoodeh, A.R., Rezaei, M. and Zendehtdel Shahri, M.R. (2016), "Linear and nonlinear torsional free vibration of functionally graded micro/nano-tubes based on modified couple stress theory", *Appl. Math. Mech. Eng. Ed.*, **37**(6), 725-740.
- Shen, H.S. (2009), "Nonlinear bending of functionally graded carbon nanotube-reinforced composite plates in thermal environments", *Compos. Struct.*, **91**(1), 9-19.
- Sun, C.H., Li, F., Cheng, H.M. and Lu, G.Q. (2005), "Axial Young's modulus prediction of single-walled carbon nanotube arrays with diameters from nanometer to meter scales", *Appl. Phys. Lett.*, **87**(19), 193101.
- Thostenson, E.T. and Chou, T.W. (2003), "On the elastic properties of carbon nanotube-based composites: Modelling and characterization", *J. Phys.-Appl. Phys.*, **36**(5), 573-582.
- Thostenson, E.T., Ren, Z.F. and Chou, T.W. (2001), "Advances in the science and technology of carbon nanotubes and their composites: A review", *Compos. Sci. Technol.*, **61**(13), 1899-1912.
- Togun, N. and Bağdatli, S.M. (2016a), "Size dependent nonlinear vibration of the tensioned nanobeam based on the modified couple stress theory", *Compos. Part B: Eng.*, **97**, 255-262.
- Togun, N. and Bağdatli, S.M. (2016b), "Nonlinear vibration of a nanobeam on a Pasternak elastic foundation based on non-local Euler-Bernoulli beam theory", *Math. Comput. Appl.*, **21**(1), 3.
- Vodenitcharova, T. and Zhang, L.C. (2006), "Bending and local buckling of a nanocomposite beam reinforced by a single-walled carbon nanotube", *Int. J. Solids Struct.*, **43**(10), 3006-3024.
- Vosoughi, A.R., Malekzadeh, P., Banan, M.A.R. and Banan, M.R. (2012), "Thermal buckling and postbuckling of laminated composite beams with temperature-dependent properties", *Int. J. Non-Linear Mech.*, **47**(3), 96-102.
- Wang, Q., Shi, D. and Liang, Q. (2016), "Free vibration analysis of axially loaded laminated composite beams with general boundary conditions by using a modified Fourier-Ritz approach", *J. Compos. Mater.*, **50**(15), 2111-2135.
- Wu, H.L., Yang, J. and Kitipornchai, S. (2016), "Nonlinear vibration of functionally graded carbon nanotube-reinforced composite beams with geometric imperfections", *Compos. Part B: Eng.*, **90**, 86-96.
- Wuite, J. and Adali, S. (2005), "Deflection and stress behaviour of nanocomposite reinforced beams using a multiscale analysis", *Compos. Struct.*, **71**(3-4), 388-396.

- Yas, M.H. and Samadi, N. (2012), "Free vibration and buckling analysis of carbon nanotube-reinforced composite Timoshenko beams on elastic foundation", *Int. J. Press. Vessels Pip.*, **98**, 119-128.
- Yazdi, A.A. (2013), "Homotopy perturbation method for nonlinear vibration analysis of functionally graded plate", *J. Vib. Acoust.*, **135**(2), 021012.
- Zafarmand, H. and Kadkhodayan, M. (2014), "Nonlinear analysis of functionally graded nanocomposite rotating thick disks with variable thickness reinforced with carbon nanotubes", *Aerosp. Sci. Technol.*, **41**, 47-54.
- Zhu, P., Lei, Z.X. and Liew, K.M. (2012), "Static and free vibration analyses of carbon nanotube-reinforced composite plates using finite element method with first order shear deformation plate theory", *Compos. Struct.*, **94**(4), 1450-1460.

CC

## Appendix A

The natural frequencies of the second-order approximation can be obtained by solving the following equation

$$\begin{aligned} & \omega^8 + \left( -\frac{25}{32}\theta_3 a^2 - \theta_1 + \frac{1}{3}\theta_2 a \right) \omega^6 \\ & + \left( \frac{3}{64}\theta_3^2 a^4 + \frac{1}{32}\theta_1 \theta_3 a^2 + \frac{5}{6}\theta_2^2 a^2 - \frac{1}{3}\theta_1 \theta_2 a - \frac{3}{4}\theta_2 \theta_3 a^3 \right) \omega^4 \\ & + \left( -\frac{9}{4096}\theta_3^3 a^6 + \frac{1}{32}\theta_3^2 \theta_2 a^5 + \frac{5}{18}\theta_2^3 a^3 - \frac{79}{96}\theta_3 \theta_2^2 a^4 \right) \omega^2 \\ & + \left( \frac{15}{512}\theta_2^2 \theta_3^2 a^6 + \frac{3}{65536}\theta_3^4 a^8 - \frac{5}{24}\theta_3 \theta_2^3 a^5 - \frac{3}{4096}\theta_2 \theta_3^3 a^7 \right) \\ & = 0 \end{aligned}$$

Also, the second-order approximation of the vibration response can be developed as

$$\begin{aligned} w_2(\tau) = \frac{1}{\omega^2} & \left[ \left( A_1 \omega^2 - \frac{A_5}{3} - \frac{A_6}{8} - \frac{A_7}{15} - \frac{A_8}{24} \right. \right. \\ & \left. \left. - \frac{A_9}{35} - \frac{A_{10}}{48} - \frac{A_{11}}{63} - \frac{A_{12}}{80} + A_{13} \right) \cos(\omega\tau) \right. \\ & + \left( \frac{A_5}{3} + A_2 \omega^2 \right) \cos(2\omega\tau) + \left( \frac{A_6}{8} + A_3 \omega^2 \right) \cos(3\omega\tau) \\ & + \frac{A_7}{15} \cos(4\omega\tau) + \frac{A_8}{24} \cos(5\omega\tau) \\ & + \frac{A_9}{35} \cos(6\omega\tau) + \frac{A_{10}}{48} \cos(7\omega\tau) + \frac{A_{11}}{63} \cos(8\omega\tau) \\ & \left. + \frac{A_{12}}{80} \cos(9\omega\tau) + A_4 \omega^2 - A_{13} \right] \end{aligned}$$

where

$$A_1 = a + \frac{\theta_2 a^2}{3\omega^2} - \frac{\theta_3 a^3}{32\omega^2}, \quad A_2 = \frac{\theta_2 a^2}{6\omega^2},$$

$$A_3 = \frac{\theta_3 a^3}{32\omega^2}, \quad A_4 = -\frac{\theta_2 a^2}{2\omega^2},$$

$$\begin{aligned} A_5 = & \frac{3}{4}\theta_3 A_2^3 + \theta_2 A_1 A_3 + \frac{1}{2}\theta_2 A_1^2 + \frac{3}{2}\theta_3 A_2 A_3^2 \\ & + \frac{3}{2}\theta_3 A_1^2 A_4 + \theta_1 A_2 + 2\theta_2 A_2 A_4 + 3\theta_3 A_2 A_4^2 \\ & + \frac{3}{2}\theta_3 A_1^2 A_2 - 4A_2 \omega^2 + 3\theta_3 A_1 A_3 A_4 + \frac{3}{2}\theta_3 A_1 A_2 A_3 \end{aligned}$$

$$\begin{aligned} A_6 = & 3\theta_3 A_3 A_4^2 + \frac{3}{4}\theta_3 A_3^3 + \frac{3}{2}\theta_3 A_2^2 A_3 + \frac{3}{4}\theta_3 A_1 A_2^2 \\ & + 3\theta_3 A_1 A_2 A_4 + \frac{3}{2}\theta_3 A_1^2 A_3 + \theta_2 A_1 A_2 \\ & + \theta_1 A_3 + \frac{1}{4}\theta_3 A_1^3 + 2\theta_2 A_3 A_4 - 9A_3 \omega^2 \end{aligned}$$

$$\begin{aligned} A_7 = & \frac{1}{2}\theta_2 A_2^2 + 3\theta_3 A_1 A_3 A_4 + \frac{3}{2}\theta_3 A_1 A_2 A_3 + \theta_2 A_1 A_3 \\ & + \frac{3}{2}\theta_3 A_2^2 A_4 + \frac{3}{4}\theta_3 A_2 A_3^2 + \frac{3}{4}\theta_3 A_1^2 A_2 \end{aligned}$$

$$A_8 = \frac{3}{4}\theta_3 A_1^2 A_3 + \frac{3}{4}\theta_3 A_1 A_2^2 + \frac{3}{4}\theta_3 A_1 A_3^2 + 3\theta_3 A_2 A_3 A_4 + \theta_2 A_2 A_3$$

$$A_9 = \frac{3}{2}\theta_3 A_1 A_2 A_3 + \frac{1}{2}\theta_2 A_2^2 + \frac{3}{2}\theta_3 A_3^2 A_4 + \frac{1}{4}\theta_3 A_3^3$$

$$A_{10} = \frac{3}{4}\theta_3 A_1 A_3^2 + \frac{3}{4}\theta_3 A_2^2 A_3$$

$$A_{11} = \frac{3}{4}\theta_3 A_2 A_3^2, \quad A_{12} = \frac{1}{4}\theta_3 A_3^3,$$

$$A_{13} = \theta_3 A_4^3 + \theta_1 A_4 + \frac{3}{2}\theta_3 A_3^2 A_4 + \frac{3}{2}\theta_3 A_2^2 A_4$$

$$+ \frac{3}{2}\theta_3 A_1 A_2 A_3 + \frac{3}{4}\theta_3 A_1^2 A_2 + \theta_2 A_4^2$$

$$+ \frac{1}{2}\theta_2 A_3^2 + \frac{1}{2}\theta_2 A_2^2 + \frac{1}{2}\theta_2 A_1^2 + \frac{3}{2}\theta_3 A_1^2 A_4$$